Preparation and Characteristics of Three Sorbents from Wood Chips Screening Reject (WCSR) Modified by Nitric Acid, Phosphoric Acid, or Sodium Hydroxide

Xiangmei Meng, Yueliang Wan, Kun Feng, Huazheng Kong, and Tingzhi Liu *

Wood chips screening rejects (WCSR) are mainly composed of sawdust, bark specks, and wood pins generated from cutting and chipping processes, as well as solid waste from pulping processes. It can be modified so that it can better serve as effective sorbents for wastewater treatment. In this study, three WCSR based sorbents were prepared by nitric acid, phosphoric acid, and sodium hydroxide treatment, respectively. The purpose of the three treatments on WCSR was to increase the specific area of WCSR, which is very essential to a high sorbent performance. It was found that nitric acid, phosphoric acid, and sodium hydroxide can be efficient modifiers of WCSR according to the results from SEM and specific area analyses, compared with those of the controls. The FT-IR results also supported the findings stated above. Thermogravimetric (TGA) analysis and X-ray diffraction (XRD) analyses were also applied to characterize the prepared sorbents. WCSR sorbents modified by the three treatments exhibited higher methylene blue adsorption values compared with that of the control sample, and that the WCSR-HNO_3 sorbent achieved the highest MB adsorption value among others, thanks to the strong acidic properties and high reactivity of HNO_3 with WCSR. The study paves a potential way to convert WCSR into effective sorbents by acid and alkali treatment.

Key words: Wood chips screening reject (WCSR); Sorbent; Modification; Nitric acid; Phosphoric acid; Sodium hydroxide; Methylene blue adsorption

*Contact information: Tianjin Key Laboratory of Pulp & Paper, Tianjin University of Science & Technology, Tianjin, 300457, China; *Corresponding author: liutz@tust.edu.cn*

INTRODUCTION

In the last decade, the wood pulping industry has entered a new phase of sustained development. One of the crucial factors that drive the recent developments in this field is the high demand of dissolving-grade pulp, as its consumption has increased from 3.3 million tons in 2007 to 6.5 million tons in 2015 in the global market (Borrega *et al.* 2018). The high demand for viscose fibers is a major contributor to the growth of dissolving pulp. The viscose fibers are the main raw material for textiles. World population growth and the increasing purchasing power of Asian markets are the main growth driving forces of the viscose fibers market. It was expected that the continued demand for viscose fibers and wood pulping would continue in the future (Liu *et al.* 2016). The other impetus for wood pulping is the application and extension of the forest-paper integrated mode in Asia, especially in China. During the processes of wood pulping, the pulp raw material preparation always generates a large amount of waste, such as sawdust and wood pins, which are eliminated *via* chip screening. As a feasible technology of solid waste recycling, reusing, and reducing, the incineration technology was the only choice available for the pulp and paper mill industry. Except for the recovery of paltry heat of combustion, the incineration technology produced many problems and negative impacts, such as environmental pollution, disturbance to energy supply system, *etc*. In this study, the WCSR was modified as an absorbent material to be used efficiently in a biomass refining concept.

As a type of paper that the mill discards, the WCSR is a type of lignocellulosic residue. The lignocellulosic residues have many advantages compared to other natural sorbents, such as low cost, great availability, and simple operational process. In recent years, researchers have made significant achievements in lignocellulosic residues adsorption, including both agricultural and wood residues. It is known that biosorption of dyes onto cellulose-related materials has the potential to minimize their release into aqueous environments, and numerous publications have described how a variety of biomass-derived substrates can be used to absorb different classes of dyestuff from dilute aqueous solutions (Hubbe *et al.* 2012). A local desert plant of Southwest Algeria and known as *Salsola vermiculata* was studied by Bestani *et al.* (2008); they showed that the plant, after its pyrolysis, was more effective for removal of methylene blue. The natural plant adsorption capacity was determined as 23 mg/g, and the corresponding results for the pyrolyzed plant uptakes were 53 mg/g. The potential of rice husk and wood chip biochars to remove levofloxacin from an aqueous solution was evaluated by Shengze *et al.* (2016). They found that the maximum Langmuir adsorption capacities of the biochars to levofloxacin (LEV) ranged from 1.49 to 7.72 mg/g and the adsorption process involved both surface adsorption and pore diffusion. In a review paper, Zhou *et al.* (2015) summarized the preparation and application of several sorbents that used the agricultural wastes as raw material and discussed the adsorption capacities for organic pollutants from aqueous solutions. The modification methods mentioned in the paper include acidification, alkaline treatment, etherification, esterification, and other methods. There is a great need for the removal of organic pollutants, such as methylene blue, by low-cost sorbents at pilot and industrial scales.

In recent years, more new technologies have been used to improve the performance of sorbents prepared from lignocellulosic residues. For example, the effect of microwave regeneration on the textural network, surface chemistry, and adsorptive properties of the agricultural waste based activated carbons was studied by Foo (2018). The sorbents prepared from lignocellulosic residues are a good choice because of the many added advantages as discussed.

In this study, three sorbents were prepared from WCSR by nitric acid, phosphoric acid, and sodium hydroxide treatment, respectively. The modified WCSR sorbents were characterized by compositional analysis, specific surface area and pore analyses, SEM analyses, FT-IR analyses, TGA and XRD analyses. Then, the prepared sorbents were respectively applied to remove the organic dye, methylene blue, from its aqueous solution.

EXPERIMENTAL

Materials

Wood chips screening reject (WCSR), generated from the process of commercial wood chips, was provided by a company of Jianghe paper in Henan province (Jianghe

Paper, Henan, China). It was mainly composed of sawdust and wood pins. The nitric acid, phosphoric acid, NaOH, and methylene blue used were all analytical grade samples.

The WCSR was first crushed with a grinder to pass through a 60-mesh sieve. Then, the WCSR powder was washed with 1:50 (g:mL) distilled water, filtered, then dried at 105 °C for approximately 6 h before use, and then was harvested and preserved as the raw material.

Preparation of WCSR-based Sorbents Modified by Nitric Acid, Phosphoric Acid and NaOH, Respectively

Preparation of nitric acid modified WCSR based sorbent (WCSR-HNO_3)

Weigh 10.00 g of dried WCSR into 250 mL iodometric flasks. Add 100 mL of 1.00 mol/L nitric acid solution, and shake at 200 rpm with a shaker at 30 °C. Modify for 2 h, filter with the Buchner funnel after the end of the shaking. Separate the modified WCSR, wash it with distilled water to near neutrality, and then dry the material to constant weight at 105 °C.

Preparation of phosphoric acid modified WCSR based sorbent (WCSR-H_3PO_4)

Weigh 10.00 g of dried WCSR into 250 mL iodometric flasks. Add 100 mL of 1.00 mol/L phosphoric acid solution, and shake at 200 rpm with a shaker at 30°C. Modify for 2 h, filter with the Buchner funnel after the end of the shaking, separate the modified WCSR, wash with distilled water to near neutrality, and then dry the material to constant weight at 105 °C.

Preparation of NaOH modified WCSR based sorbent (WCSR-NaOH)

Weigh 10.00 g of dried WCSR into 250mL iodometric flasks. Add 100 mL of 1.00 mol/L NaOH solution, and shake at 200 rpm with a shaker at 30°C. Modify for 2 h, filter with the Buchner funnel after the end of the shaking, separate the modified WCSR, wash with distilled water to near neutrality, and then dry the material to constant weight at 105 °C.

Characteristics of WCSR Sorbents

Compositional analyses of original and modified WCSR

Conventional characteristics of the WCSR, such as the benzene-alcohol extracts, acid insoluble lignin, and acid soluble lignin, were determined based on the traditional standard measurements. The contents of cellulose and hemicellulose were determined *via* a previously reported method (Jin *et al.* 2017). The conventional characteristics of the original and modified WCSR are shown in Table 1.

Analysis of specific surface area and pore characteristics

The pore structure of WCSR, such as specific surface area and pore size distribution, was analyzed by N_2 adsorption-desorption process using Autosorb-iQ automatic specific surface and pore size distribution analyzer.

SEM analyses

The WCSR was taken and made into slices and sprayed with gold according to the requirements. The surface morphology of sawdust was observed by JSM-IT300LV scanning electron microscope and photographed.

FT-IR analyses

The surface functional groups of WCSR were qualitatively determined by FTIR-650 infrared spectrometer (Tianjin Gangdong Sci. & Tech. Development Co., Ltd., Tianjin, China) using potassium bromide tablet method. A small amount of WCSR was weighed and placed in an agate mortar, and the dried potassium bromide was added in the proportion of 1:100 for full grinding. Then the transparent sheets were pressed by a tablet press and analyzed by Fourier transform infrared spectroscopy.

TGA analyses

Thermogravimetric analysis was conducted using a TGA Q500 thermogravimetric analyzer (TA Instruments, Tianjin, China)

XRD

An XRD-6100 X-ray diffractometer (Jcnano, Tianjin, China) was employed for XRD analysis with a scanning range of 2θ = 10° to 80° and a scanning speed of 2 °/min.

Methylene blue adsorption value tests

First prepare a 1.5 g/L methylene blue solution. Then remove 50 mL of 1.5 g/L methylene blue solution to a 1000 mL volumetric flask and dilute to the calibration line. This makes a 75 mg/L methylene blue solution. Move 0.5 mL, 1.0 mL, 1.5 mL, 2.0 mL, 2.5 mL, 3.0 mL, 3.5 mL, 4.0 mL, 4.5 mL, and 5.0 mL to a series of test tubes, dilute to the calibration line with buffer solution, and then obtain the standard absorption curve of methylene blue solution at 665 nm.

The methylene blue adsorption value of the original and modified WCSR samples were determined according to the method of Danish *et al.* (2018). Weigh 0.1000 g of WCSR and place it in 250 mL iodometric flasks, adding 10 mL of 1.5 g/L methylene blue solution to wet all the samples. Observe the color change of methylene blue. If the color fades quickly, then add a sufficient amount of additional methylene blue solution. Shake gently, confirming that the solution still remains a slightly blue. Place the above solution in a shaker, with a temperature setting of 25 °C, rotational speed of 200 rpm, and time of 20 min. After the oscillation, filter the mixture, and evaluate the light absorbance of the filtrate at 665 nm. Results from the methylene blue adsorptions are shown in Table 3.

RESULTS AND DISCUSSION

Components Analyses

The WCSR sample used in this study was collected from an alkaline peroxide mechanical pulp (APMP) plant in China. The lignin content of WCSR used was comparable to that of hard wood. Kraszkiewicz *et al.* (2015) found that the content of cellulose of buckwheat straw pellets is 31.8% and that the total of hemicellulose plus lignin was approximately 52.4%. The conventional cellulose content of wood chips was approximately 40% to 45%, but it was only 38% in WCSR, which can be explained by two primary factors. One was that there were some bark and saw dust that were found in the WCRS. The other factor was that the mixing of some brushwood in WCSR could lead to the decrease of cellulose content. Raud *et al.* (2016) found that the cellulose content of sunflower was approximately 34.1%, which was closer to the cellulose content of WCSR. The hemicellulose and lignin contents in WCSR were 5.2% and 7.7%, respectively, which were largely deviated from those of WCSR. The organic content of phenyl alcohol extracted was 1.9%. This was about double that of non-wood pulp materials, such as wheat straw (Lauberts *et al.* 2018). From Table 1, the ash content of WCSR was 2.2%, in accordance with the vast majority wood pulp materials.

Table 1. Conventional Indexes of Original and Modified WCSR

	Organic Extracts (%)	Cellulose (%)	Hemicellulose (%)	Lignin (%)
Original	1.880	38.50	32.00	24.00
WCSR-HNO_3	1.720	32.24	22.68	20.06
WCSR-H_3PO_4	1.940	37.30	26.66	21.44
WCSR-NaOH	2.000	37.76	31.42	23.96

As shown in Table 1, the cellulose, hemicellulose, and lignin contents of modified WCSR showed different degrees of reduction compared to the original. This indicated that these samples could be easily dissolved under acid-base conditions. However, the three main constituents of WCSR-NaOH were very close to those of original WCSR. This could be that the dissolution rate of NaOH treatment at room temperature was imperceptible.

Pore Size/ Porosity Analyses

The specific surface area and pore size distributions of the original and modified WCSR were examined and the results are shown in Table 2. The specific surface areas of the three modified WCSR samples increased noticeably. However, the pore volumes of the HNO_3 and NaOH solution modified samples decreased dramatically. This can be explained by the increased crystallinity of these samples after modification, which resulted in the decrease of pore volumes. The increase of average pore size volume may be related to osmotic swelling of NaOH solution. Chen *et al.* (2018) explored the pore characteristics and fractal properties of biochar obtained from the pyrolysis of coarse wood in a fluidized-bed reactor. Most of the pores in the coarse wood were mesoporous with diameters between 2 nm and 10 nm. In this study, the average pore size of the original and modified WCSR was also between 2 nm and 10 nm.

Table 2. Specific Surface Area, Pore Volume, and Average Pore Size Values of Original and Modified WCSR

	Specific Surface Area (m^2/g)	Pore Volume (mL/g)	Average Pore Size (nm)
Original	7.699	$8.059*10^{-2}$	3.625
WCSR-HNO_3	14.15	$4.555*10^{-2}$	3.627
WCSR-H_3PO_4	11.75	$8.536*10^{-2}$	3.630
WCSR-NaOH	10.47	$3.864*10^{-2}$	4.628

The modification conditions used in this study were room temperature and a low chemical concentration. Therefore, the treatment process can be defined as a surface modification. Moreover, the modified treatments had less destruction and influence on the structure of WCSR.

SEM Analyses

The SEM micrographs of the original and the three modified WCSR samples are shown in Fig. 1. The surface structure of WCSR was rough, the pore structure was very obvious and loose, its shape was irregular, and its size was diverse. It can be observed from Fig. 1 that the diameters in the porous structure of WCSR were about 5 microns. The pore sizes of WCSR-HNO_3 and WCSR-H_3PO_4 were increased to 10 microns. This may be due to the dissolution or ablation of particles such as inorganic fillers attached to the surface of fibers during impregnation activation, or the chemical reactions of HNO_3, H_3PO_4 and WCSR, resulting in a large number of porous structures, or fractures occurring in some parts and a large number of mesoporous micropores are formed by ablation and collapse. Although these pore structures cannot directly improve the adsorption performance of WCSR, they can provide more permeation channels for the adsorption of mesoporous or microporous, thus improving the adsorption efficiency of WCSR. However, the pore size structure of WCSR-NaOH was not changed significantly. As shown in Fig. 1, mesoporous structure can be clearly observed near the macropore, which is basically consistent with the pore size measured by N_2 adsorption-desorption.

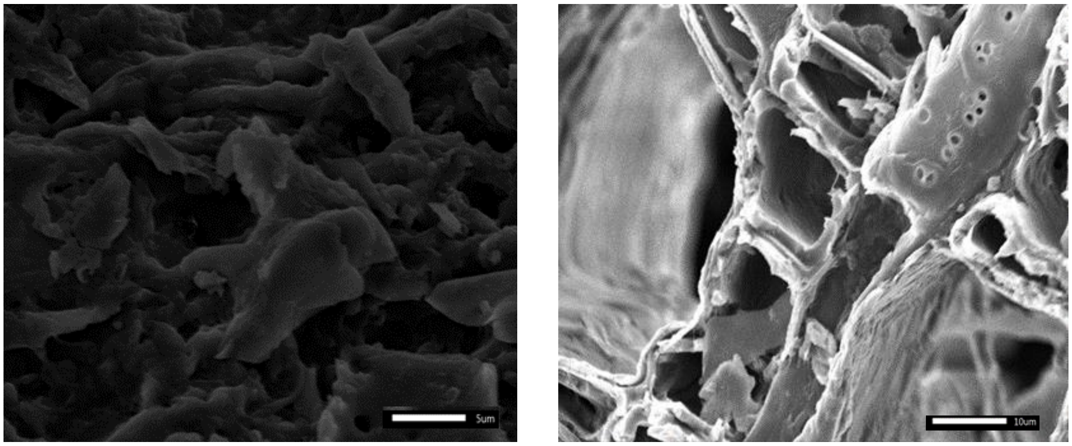

WCSR
(a)

WCSR-HNO_3
(b)

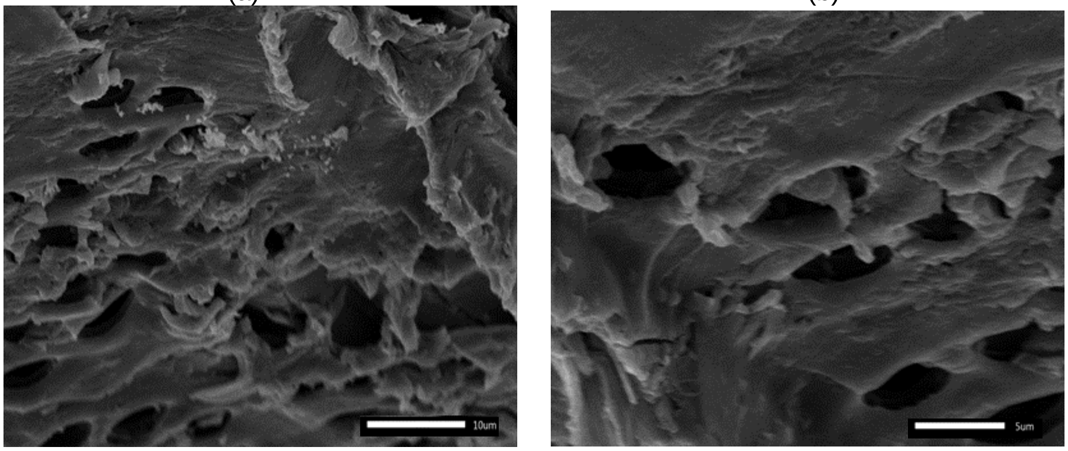

WCSR-H_3PO_4
(c)

WCSR-NaOH
(d)

Fig. 1. SEM analysis of original and modified WCSR

FT-IR Analyses

Results of infrared scans of the original and the three modified WCSR samples are shown in Fig. 2. According to the analysis, the main functional group on the surface of the WCSR samples is a hydroxyl (-OH) group. The broad absorption peak at 3400 cm^{-1} was mainly caused by the O-H stretching vibration (Yu *et al.* 2015). This is because of the fact that the WCSR is mainly composed of cellulose and hemicellulose components, and the contents of these two components was approximately 70%. Furthermore, Fig. 2 also indicates that the absorption peaks of the hydroxy groups of modified WCSR samples had been enhanced. The structural modifications of *Tilia cordata* wood during heat treatment were studied by Popescu *et al.* (2013) and they have observed IR bands corresponding to intermolecular hydrogen bonds involving the C6 position (primary hydroxyl groups) at 3430 cm^{-1}, which were responsible for the formation of crystalline regions in the cellulose component of wood. Therefore, the enhancing of –OH band absorption peaks revealed that the degree of crystallinity of modified WCSR was increased, which improved the structural stability of modified WCSR. As an absorbent, high structural stability implies a good property. The presence of a new absorption peak at 1750 cm^{-1} in WCSR-HNO_3 and WCSR-H_3PO_4 demonstrated the formation of a -C=O group (Popescu *et al.* 2011) resulting from the reaction of the acid and the hydroxyl groups on the WCSR surface. The absorption peak of the -C=O group formed by WCSR-HNO_3 was more intense, which enhanced the adsorption capability (Jia *et al.* 2009). A small -C-H stretching vibration peak appeared near 2600 cm^{-1} in the WCSR-NaOH, and the peaks at 1268 cm^{-1}, 1900 cm^{-1}, 1511 cm^{-1}, and 1735 cm^{-1} disappeared, indicating the rupture of structures containing -C-O-H and -C=C groups (Zhang et *al.* 2017).

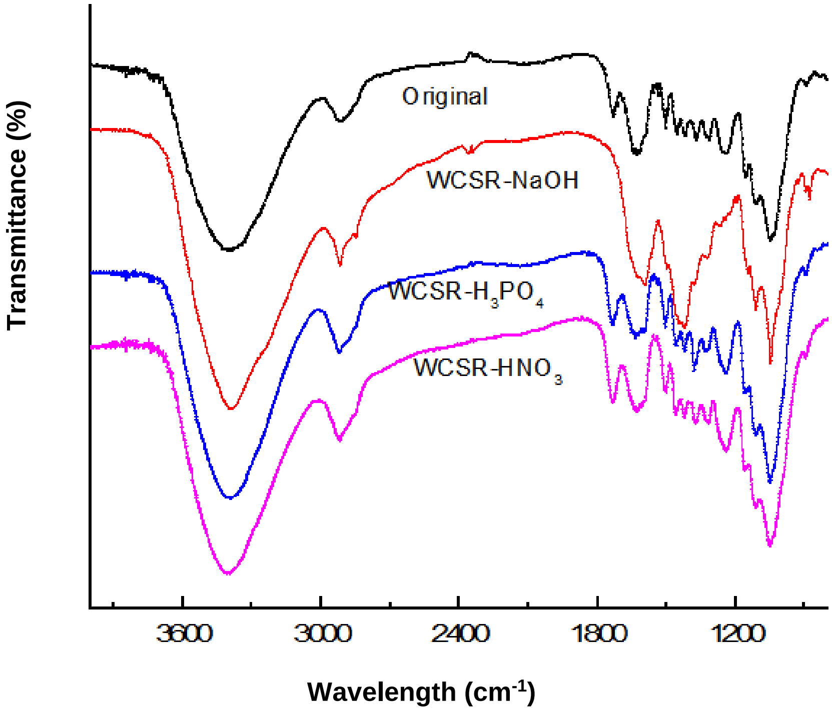

Fig. 2. IR spectra of original and modified WCSR

TGA Analyses

Thermal stabilities of the original and modified WCSR samples were studied, and the thermogravimetric (TG) and differential thermogravimetric (DTG) curves are shown in Fig. 3. The pyrolysis or thermal reactions of the original, WCSR-HNO_3 and WCSR-H_3PO_4 can be divided into two stages: (1) from room temperature to 105 °C, which revealed the loss of the remaining water and volatile substances. The TG curve (Fig. 3a) indicated the weight loss of samples with temperature; (2) from 250 °C to 500 °C, which displayed the biomass pyrolysis stage, where the biomass conversion and dissociation stage occurred. As shown in Fig. 3, the temperature at which the severe weight loss of the original WCSR occurred at was approximately 350 °C.

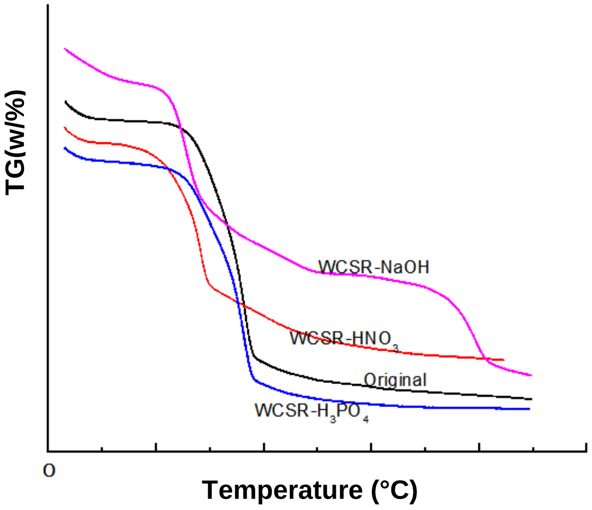

(a)

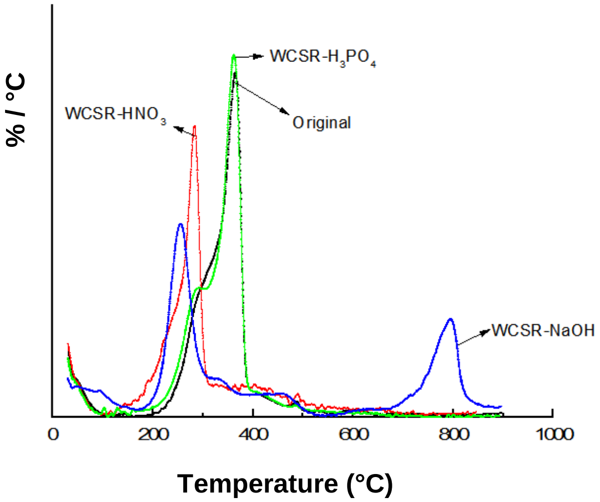

(b)

Fig. 3. TG (a) and DTG (b) analyses of original and modified WCSR

The weight loss temperatures of WCSR-HNO_3 and WCSR-H_3PO_4 were approximately 250 °C and 300 °C, respectively. The weight loss temperature of the WCSR-HNO_3 and WCSR-H_3PO_4 was lower than that of the original WCSR. This was explained by the fact that the esterification reaction of the acid and the hydroxyl groups led to the decline of thermal stability of modified WCSR. In this stage, the organic materials of the WCSR were pyrolyzed rapidly and gases, such as CO_2 and CO, were generated. This was attributed to the total pyrolysis of cellulose and hemicellulose, and the pyrolysis of some lignin to generate volatile gases. In addition to the above two stages, there was also a peak at 800 °C that was related to the weight loss peak of the WCSR-NaOH, and represented the decomposition of inorganic substances. These results were comparable to those reported earlier in literature by Wang *et al.* (2014), where the pyrolysis of milled wood lignin was divided into three stages. In the second stage, from 160 °C to 500 °C, the main structure of lignin was broken and corresponded to the major weight loss. Yang *et al.* (2012) discussed the pyrolysis process of pine wood chips, which was generally consistent with the changing trend found in this study. Song and Hu (2003) found that the main pyrolysis of straw occurred from 200 °C to 400 °C. The pyrolysis characteristics of hemicellulose, cellulose, and lignin are very different, and the pyrolysis of hemicellulose mainly occurs at 250 °C to 340 °C, for cellulose it is in the range of 300 °C to 400 °C, and lignin pyrolysis has a relatively wide range.

XRD

The crystal structures of the original and modified WCSR samples were determined using XRD analysis and the spectra are shown in Fig. 4.

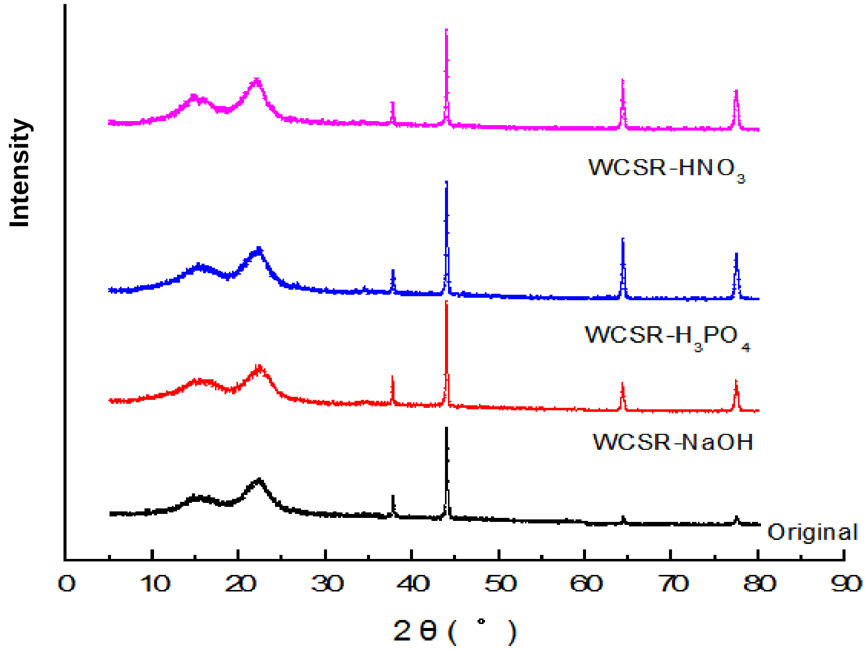

Fig. 4. XRD analysis of original and modified WCSR

There were two distinct diffraction peaks in the XRD spectrum of the original WCSR. The broad diffraction peak between 20° and 28° and a strong peak at around 44° were found. These peaks represent the (002) and the (100) crystal planes of the WCSR (Liu *et al.* 2014). The higher intensity of the (100) diffraction peak (Lu 2001) indicates that the graphitization of the WCSR was deeper and the pore structure was more stable. The (002) peak is diffusive (Kraus *et al.* 1997; Yoshizawa *et al.* 2002), indicating that the WCSR had a large degree of crystallization. It further shows that the crystallites were very irregular, and there were a large number of pore structures with different shapes and sizes that exist in WCSR. This will better ensure the stability of the WCSR. There was no obvious change in the X-ray spectrum of WCSR after modification. This further showed that the modified conditions were mild. The modification affected only the cellulose surface but did not affect the crystal structure of the WCSR.

Methylene Blue Adsorption Analyses

Table 3 shows that the methylene blue adsorption values of the WCSR samples were improved considerably after the modification treatments. The methylene blue adsorption values of WCSR modified by nitric acid, phosphoric acid, and NaOH solution improved by 366.6%, 250.0%, and 133.3%, respectively, compared to the original WCSR without modification. The adsorptive property value of nitric acid modification was the most noticeable in the three modified methods, while the NaOH solution treatment had the lowest effect on the adsorptive property. Bestani *et al.* (2008), investigated the adsorption ability of a desert plant (*Salsola vermiculata*) for methylene blue and iodine, where the methylene blue and iodine adsorption capacities of the natural plant were 23 mg/g and 272 mg/g, respectively. The values of WCSR-HNO_3 and WCSR-H_3PO_4 (modification time 2 h) reached 42.0 mg/g and 31.5 mg/g. The results from the present study are comparable to the findings of Batzias and Sidiras (2007), in which pine wood chips were modified with acid solution and the maximum values of methylene blue adsorption reached were 13.7 mg/g and 30.5 mg/g after 1 h and 4 h of modification treatment.

Table 3. Methylene Blue Adsorption Values of Original and Modified WCSR

	Methylene Blue Adsorption (mg/g)
Original	9.0
WCSR-HNO_3	42.0
WCSR-H_3PO_4	31.5
WCSR-NaOH	21.0

CONCLUSIONS

1. Conventional compositional analysis established that the content of cellulose in WCSR was lower than that in pulping chips and the contents of other components in WCSR were similar to the pulping chip materials.
2. The modifications can be regarded as surface modifications, and have less destruction and influence on the structure of WCSR.

3. The room-temperature modifications had remarkable effects on the functional groups of the WCSR surface, thus improving the adsorption performance of modified WCSR.
4. Comparing the adsorption performance of sorbents by the three modified methods, the nitric acid modification had the best effect on the WCSR, while the NaOH solution modification had a small effect on adsorption.

REFERENCES CITED

Batzias, F. A., and Sidiras, D. K. (2007). "Dye adsorption by prehydrolysed beech sawdust in batch and fixed-bed systems," *Bioresource Technology* 98(6), 1208-1217. DOI: 10.1016/j.biortech.2006.05.020

Bestani, B., Benderdouche, N., Benstaali, B., Belhakem, M., and Addou, A. (2008). "Methylene blue and iodine adsorption onto an activated desert plant," *Bioresource Technology* 99(17), 8441-8444. DOI: 10.1016/j.biortech.2008.02.053

Borrega, M., Larsson, P. T., Ahvenainen, P., Ceccherini, S., Maloney, T., Rautkari, L., and Sixta, H. (2018). "Birch wood pre-hydrolysis *vs* pulp post-hydrolysis for the production of xylan-based compounds and cellulose for viscose application," *Carbohydrate Polymers* 190, 212-221. DOI: 10.1016/j.carbpol.2018.02.064

Chen, J., Fang, D. D., and Duan, F. (2018). "Pore characteristics and fractal properties of biochar obtained from the pyrolysis of coarse wood in a fluidized-bed reactor," *Applied Energy* 218, 54-65. DOI: 10.1016/j.apenergy.2018.02.179

Danish, M., Ahmad, T., Hashim, R., Said, N., Nishat, M., Akhtar, Mohamad, S. J., and Sulaiman (2018). "Comparison of surface properties of wood biomass activated carbons and their application against rhodamine B and methylene blue dye," *Surfaces and Interfaces* 11, 1-13. DOI: 10.1016/j.surfin.2018.02.001

Foo, K. Y. (2018). "Effect of microwave regeneration on the textural network, surface chemistry and adsorptive property of the agricultural waste based activated carbons," *Process Safety and Environmental Protection* 116, 461-467. DOI: 10.1016/j.psep.2018.01.022

Hubbe, M. A., Beck, K. R., O'Neal, W. G., and Sharma, Y. C. (2012). "Cellulosic substrates for removal of pollutants from aqueous systems: A review. 2. Dyes," *BioResources* 7(2), 2592-2687. DOI: 10.15376/biores.8.2.3038-3097

Jia, J. G., Li, C., Zhu, C. L., Xiao, C. Y., Xu, D.,Yan, X., and Liang, C. H. (2009). "Surface modification of activated carbon with nitric acid and its adsorption properties," *Carbon Techniques* 6, 12-13. DOI: 10.14078/j.cnki.1001-3741.2009.06.005

Jin, X. L., Chen, X. L., Shi, C. H., Li, M., Guan, Y. J., Yu, C. Y., Yamada, T., Sacks, E. J., and Peng, J. H. (2017). "Determination of hemicellulose, cellulose and lignin content using visible and near infrared spectroscopy in *Miscanthus sinensis*," *Bioresource Technology* 241, 603-609. DOI: 10.1016/j.biortech.2017.05.047

Kraszkiewicz, A., Kacheljakubowska, M., Lorencowicz, E., and Przywara, A. (2015). "Influence of cellulose content in plant biomass on selected qualitative traits of pellets," *Agriculture and Agricultural Science Procedia* 7, 125-130. DOI: 10.1016/j.aaspro.2015.12.005

Kraus, J. F., Benson, C. H., Maltby, C. V., and Wang, X. (1997). "Laboratory and field hydraulic conductivity of three compacted paper mill sludges," *Journal of Geotechnical & Geoenvironmental Engineering* 123(7), 654-662.

Lauberts, M., Lauberte, L., Arshanitsa, A., Dizhbite, T., Dobele, G., Bikovens, O., and Telysheva, G. (2018). "Structural transformations of wood and cereal biomass components induced by microwave assisted torrefaction with emphasis on extractable value chemicals obtaining," *Journal of Analytical and Applied Pyrolysis* (In press). DOI: 10.1016/j.jaap.2018.03.025

Liu, B. S., Wang, W. S., Wang, N., and Au, C. T. (2014). "Preparation of activated carbon with high surface area for high-capacity methane storage," *Journal of Energy Chemistry* 23(5), 662-668. DOI: 10.1016/S2095-4956(14)60198-4

Liu, Y., Shi, L., Cheng, D., and He, Z. (2016). "Dissolving pulp market and technologies: Chinese prospective–A mini-review," *BioResources* 11(3), 7902-7916. DOI: 10.15376/biores.11.3.7902-7916

Lu, A .H., and Zheng, J. T. (2001). "Study of microstructure of high-surface-area polyacrylonitrile activated carbon fibers," *Journal of Colloid and Interface Science* 236(2), 369-374. DOI: 10.1006/jcis.2000.7425

Popescu, M. C., Froidevaux, J., Navi, P., and Popescu, C. M. (2013). "Structural modifications of *Tilia cordata*, wood during heat treatment investigated by FT-IR and 2D IR correlation spectroscopy," *Journal of Molecular Structure* 1033, 176-186. DOI: 10.1016/j.molstruc.2012.08.035

Popescu, C. M., Popescu, M. C., and Vasile, C. (2011). "Structural analysis of photodegraded lime wood by means of FT-IR and 2D IR correlation spectroscopy," *International Journal of Biological Macromolecules* 48(4), 667-675. DOI: 10.1016/j.ijbiomac.2011.02.009

Raud, M., Tutt, M., Olt, J., and Kikas, T. (2016). "Dependence of the hydrolysis efficiency on the lignin content in lignocellulosic material," *International Journal of Hydrogen Energy* 41(37), 16338-16343. DOI: 10.1016/j.ijhydene.2016.03.190

Song, C., and Hu, H. (2003). "Catalytic pyrolysis and kinetics of straw and its main components," *Coal Conversion* 26(3), 91-97.

Wang, S. R., Lin, H. Z., Ru, B., Su, W. X., Wang, Y. R., and Luo, Z. Y. (2014). "Comparison of the pyrolysis behavior of pyrolytic lignin and milled wood lignin by using TG-FTIR analysis," *Journal of Analytical and Applied Pyrolysis* 108, 78-85. DOI: 10.1016/j.jaap.2014.05.014

Yang, X., Chai, Y., and Chen, Y. (2012). "Study on non-isothermal kinetics of pine sawdust pyrolysis," *Henan Science* 30(8), 1024-1028.

Yoshizawa, N., Maruyama, K., Yamada, Y., Ishikawa, E., Kobayashi, M., Toda, Y., and Shiraishi, M. (2002). "XRD evaluation of KOH activation process and influence of coal rank," *Fuel* 81(13), 1717-1722. DOI: 10.1016/S0016-2361(02)00101-1

Zhang, Z. Z., Zhu, M. M., and Zhang, D. K. (2017). "Pyrolysis characteristics of cellulose isolated from selected biomass feedstocks using a thermogravimetric analyser," *Energy Procedia* 142, 636-641. DOI: 10.1016/j.egypro.2017.12.105

Zhou, Y., Zhang, L., and Cheng, Z. J. (2015). "Removal of organic pollutants from aqueous solution using agricultural wastes: A review," *Journal of Molecular Liquids* 212(9), 739-762. DOI: 10.1016/j.molliq.2015.10.023

Article submitted: July 31, 2018; Peer review completed: October 20, 2018; Revised version received: January 18, 2019; Accepted, January 19, 2019; Published: January 30, 2019.
DOI: 10.15376/biores.14.1.2216-2228